

Stiffness of Substrate Influences the Distribution but not the Synthesis of Autophagosomes in Human Liver (LO2) Cells

Fang Xu^{1,2}, Yue Wang³, Mingzhi Luo¹, Yan Pan¹, Haowen Li⁴, Yajie Wang⁴, Guohua Qiu¹ and Linhong Deng^{1,3,*}

¹Institute of Biomedical Engineering and Health Sciences, Changzhou University, Changzhou, Jiangsu 213164, China

²School of Pharmaceutical Engineering and Life Science, Changzhou University, Changzhou, Jiangsu 213164, China

³School of Nursing, Changzhou University, Changzhou, Jiangsu 213164, China

⁴Laboratory of Clinical Medical Research, Beijing Tiantan Hospital, Capital Medical University, Beijing 10050, China

Abstract: Extracellular matrix (ECM) often becomes stiffer during tumor development, which not only gives the tumor's hardness feel but also actively contributes to the tumor formation. A good example is hepatocellular carcinoma (HCC) that usually develops within chronically stiffened liver tissues due to fibrosis and cirrhosis. On the other hand, HCC cells exhibit reduced autophagy in a malignancy dependent manner, suggesting autophagy is suppressed during tumor development. However, it is not known whether ECM stiffness would influence autophagy during tumor development. To investigate this issue, We cultured the human liver (LO2) cells that stably expressed autophagosome indicator LC3 on polydimethylsiloxane (PDMS) gels with stiffness varying from 11 to 1220 kPa. and on plastic cell culture dish as controls for up to 48h. We found that the total protein level of LC3-II in LO2 cells was not affected by the substrate stiffness. However the autophagosomes in LO2 cells cultured on the soft substrate (11 kPa PDMS gel) were localized and accumulated around the nucleus, while those on the stiff substrate (1220 kPa PDMS gel or plastic dish surface) were dispersed throughout the cytoplasmic space. Therefore, our data suggest that ECM stiffness may not directly synthesize nascent autophagosomes, but instead influence the location/translocation and ultimately distribution of autophagosomes in the cells.

Keywords: Hepatic cells, Substrate stiffness, Autophagy, Cirrhosis, Translocation.

1. INTRODUCTION

Hepatocellular carcinoma (HCC) is one of the most common cancers with more than 700,000 cases diagnosed yearly, and the third leading cause of cancer-related death worldwide [1]. Interestingly, the majority of HCC are known to be the progressive outcomes of liver fibrosis and cirrhosis, an established chronic liver disease characterized by stiffening of liver tissue [1-3]. Normal liver tissue is very soft, of which the elastic modulus is typically between 300 and 600 Pa. However, when the liver develops fibrosis and cirrhosis, its stiffness can increase to 20 kPa or beyond [4, 5]. This pathological stiffening of liver tissue is largely attributable to increase of stiffness of the extracellular matrix (ECM).

Previous studies have shown that changes of ECM structure or mechanical properties, particularly the stiffness (resistance to deformation) can exert great influence on the cells residing within, including broad

regulation of cell signaling [6], determination of cell phenotype [7], facilitation of cell adherence and growth [8], and even active contribution to tumor formation [9, 10]. Therefore, ECM or substrate stiffness is increasingly appreciated as an important mediator of cell behaviors either *in vitro* or *in vivo*.

On the other hand, recent data demonstrated that pathogenesis of hepatology involves autophagy that is the primary intracellular degradation system by which cytoplasmic materials are delivered to and degraded in the lysosome [11, 12]. There are about three classes of autophagy, namely microautophagy, chaperone-mediated autophagy, and macroautophagy. Here we will focus on macroautophagy (hereafter referred to as autophagy). Macroautophagy uses intermediate organelle autophagosomes to capture and degrade waste materials in the cytoplasm. The process starts with the formation of a small vesicular called isolation membrane or phagophore that then elongates and subsequently encloses a portion of cytoplasm into a double membraned phagophore [13]. The double membraned phagosome encircles degradable cellular components, such as misfolded proteins, damaged organelles or recyclable cytoplasmic constituents, and

*Address correspondence to this author at the Institute of Biomedical Engineering and Health Sciences, Changzhou University, 1 Gehu Road, Wujin District, Changzhou, Jiangsu, 213164 China; Tel: +86 (519) 86330988; Fax: (86) 0519-86330988; E-mail: dlh@cczu.edu.cn

forms an autophagosome. Then, the outer membrane of the autophagosome fuses with a lysosome to form an autolysosome, leading to the degradation of the enclosed materials together with the inner autophagosomal membrane. Amino acids and other small molecules that are generated by autophagic degradation are delivered back to the cytoplasm for either recycling or energy production [14].

In normal conditions and most liver diseases, autophagy provides a protective function for the liver tissue. For example, in fatty liver disease autophagy protect the liver from lipid accumulation by degrading the lipid droplets in the hepatic cells [15]. In some liver diseases, however, the autophagy is impaired for various reasons so that the autophagy-mediated protection is hampered. For example, during hepatitis B or C infection, autophagy is subverted by viruses to promote their own replication [16], and in HCC tissues or cell lines the autophagic level is progressively reduced as the malignancy level of the tissue or cells enhanced, especially when the anti-apoptotic B-cell leukemia/lymphoma (Bcl)-xL protein is over-expressed [17]. Pharmacological agents such as rapamycin, tamoxifen, carbamazepine, sodium valproate and lithium, cisplatin have been found to induce or stimulate autophagy, whereas vinblastine, antimalarial compounds chloroquine and hydroxychloroquine as well as the antidepressant agent clomipramine are known to inhibit this process [18-20].

Although both ECM stiffness, and autophagy has been directly implicated in the pathogenesis of cancers in general, and HCC in particular [21, 22], their functions have usually been studied separately and much has been learned of ECM stiffness and autophagy as independent contributing factors to HCC. Much less is known, however, whether autophagy process would be dependent on the ECM stiffness, which may be hypothesized as a molecular mechanism for the liver cells to sense external physical cues of the ECM and correspondingly regulate the biological processes inside the cell. To address this question, we investigated the autophagy behavior of normal human liver (LO2 cell line) cells versus the stiffness of polydimethylsiloxane (PDMS) substrate on which the cells were cultured. The stiffness of the PDMS varied from 11 to 1220 kPa, and plastic Petri dish was used as control of rigid substrate. LO2 cells were cultured on these substrates for up to 48h. Subsequently, the cells were examined by florescent microscopy to identify and locate the LC3-labelled autophagosomes inside the cells, and by Western blot to quantify the protein expression level of LC3-II, respectively. The results

showed that the total protein level of LC3-II in LO2 cells was not affected by the substrate stiffness. However, the autophagosomes in LO2 cells cultured for 48h on the soft substrate (11 kPa PDMS gel) became localized and accumulated around the nucleus, while those on the stiff substrate (1220 kPa PDMS gel or plastic dish surface) were dispersed throughout the cytoplasmic space. Quantitatively, the number of cells with autophagosomes accumulated around the nuclei increased more than 6 fold as the substrate stiffness decreased from 1220 to 11 kPa. Thus it was demonstrated that ECM stiffness influenced not the amount but the distribution of autophagosomes in the cells, which provides the first evidence of physical regulation of autophagy as complementary to the well-known chemical regulations. This may not only help better understand the molecular mechanism between ECM stiffness and autophagy but also provide insight for developing new therapeutic target aiming at autophagy in liver disease.

2. MATERIALS AND METHODS

2.1. Chemicals and Reagents

pcDNA3-GFP, pcDNA3-GFP-LC3 plasmid (a gift of Peking University; Beijing, China). Normal human liver cell line LO2 (a gift of East China University of Science and Technology; Shanghai, China). Dulbecco's modified Eagle's medium (DMEM). Neomycin (G418), rapamycin were purchased from SIGMA (St. Louis, MO). Fetal bovine serum (FBS), Opti-MEM was purchased from Gibco (North Andover, MA). Translipid transfection reagent was purchased from TransGen (Beijing, China). Anti-LC3B was purchased from Novus (Colorado, USA). Anti- β -actin was purchased from CWBIO (Beijing, China). Anti-rabbit IgG was purchased from LI-COR (Nebraska, NV).

2.2. Cell Culture and Transfection of GFP-Tagged LC3 Expression Vector

LO2 cells (4×10^5 cells/well) were plated onto the cell culture Petri dish and maintained in DMEM containing 10% FBS. After 24 hours of cultivation, the cells were transfected with pcDNA3-GFP, pcDNA3-GFP-LC3 plasmid using the translipid transfection reagent. Serial cultures were performed according to the manufacturer's instructions.

2.3. Selection of LO2 Cells Stably Expressing LC3

Because pcDNA3-GFP, pcDNA3-GFP-LC3 have the neomycin (G418) resistance marker (NeoR), cells

without transfection of pcDNA3-GFP, pcDNA3-GFP-LC3 would not survive when exposed to G418. So we added G418 in the culture medium to selectively screen positive clones of LO2 cells. Instead of using conventional method, here we established a simple, new and high throughput method to generate cells stably expressing LC3 as follows. First, the cells were cultured in 96-well cell culture plate and transfected with GFP-tagged LC3. After 16h transfection, the cells were harvested by trypsinization. After brief wash and resuspension into cell culture medium, the cells were replaced into the 96-well plate at three different cell density. As illustrated in Figure 1A, the 96-well plate was divided into three parts, each with 4 columns of wells. Cells were seeded into the 4 columns on the left, middle, and right at the density of 2000, 1000, and 500 cells/well, respectively, with 280 μ L medium containing 400 μ g/mL G418. After 15 d in culture, non-transfected cells would die out, because of the presence of G418 in the medium, but transfected cells would survive and grow into clone(s) in the well. The cells grown into two or more clones as shown in Figure 1B were discarded, and only cells grown into a single clone in one well as shown in Figure 1C/D were selected and harvested by trypsinization. In this way, multiple monoclonal cells expressing GFP-tagged LC3 could be obtained from each batch of 96-well plates. And these monoclonal cells were then further expanded by culturing in 24-well cell culture plate.

2.4. Preparation of PDMS Gel Substrates with Varying Stiffness

PDMS used in the present work is a liquid bi-component silicone pre-polymer. The stiffness of the PDMS gel can be controlled by the concentration of cross-linker (curing) agent in the PDMS solution, the temperature and time of curing. We prepared the PDMS solutions with mixture of curing agent/PDMS polymer at concentration of 0.2:10, 0.3:10, 1:10 (w/w), respectively. The PDMS solutions were first leveled for 30 min at room temperature, and then baked at constant temperature of 100 $^{\circ}$ C until proper gel stiffness was achieved. In order to ensure cell adhesion and growth on the PDMS substrate, the surface of the PDMS gel was plasma oxidized to render it hydrophilic, and then coated with rat tail collagen Type I (1 mL at 0.01 mg/mL) overnight at 4 $^{\circ}$ C.

The stiffness, or Young's modulus of the prepared PDMS gel was measured by atomic force microscopy (AFM), using NanoWizard 3 (JPK, Jena, Germany).

Briefly, V-shaped silicon nitride cantilevers (MLCT, Bruker, Camarillo, CA) with a nominal spring constant of 0.06 N m $^{-1}$ were utilized in all measurements. The spring constant of the cantilever was determined using the thermal noise method [23]. A cantilever tip of pyramidal shape with a half opening angle of 35 $^{\circ}$ was used to probe the substrate. The tip was indented into the PDMS substrate at a rate of 2.5 μ m s $^{-1}$ to produce a force-distance curve. Young's modulus, or stiffness of the substrate was calculated from the force curves according to Hertz model [24]. The Hertz model described the elastic deformation of a soft sample by a stiff cone using the following equation

$$F = \left(\frac{E}{1-\nu^2} \right) \frac{2 \tan \alpha}{\pi} \delta^2$$

Where F was the loading force, E was the Young's modulus, ν was the Poisson's ratio ($\nu = 0.5$), α was the half-opening angle of the pyramidal tip (in the case of SixNy tips used in this study, $\alpha = 35^{\circ}$) and δ was the depth of indentation into the sample. All experiments were performed in distilled water at room temperature.

2.5. Induction of Autophagy in LO2 Cells

It is known that intracellular autophagy can be induced by either serum starvation, or drug treatment with rapamycin or NH $_4$ Cl. Thus the LC3-expressing LO2 cells were treated either with serum starvation, or rapamycin with/out NH $_4$ Cl to induce autophagy in the cells. However, before the treatment, the LO2 cells were first incubated in DMEM for 3h. Then the cells were washed and further incubated in Opti-mem, DMEM with 10 μ M rapamycin, DMEM with 10mM NH $_4$ Cl, DMEM with 10 μ M rapamycin together with 10mM NH $_4$ Cl, respectively, for additional 4h. Cells incubated in complete medium for the same time were used as controls.

LO2 cells stably expressing LC3 were plated onto PDMS substrates of various stiffness and the plastic surface of Petri dish, then treated either with serum starvation or drug to induce autophagy as described above. Consequently, the induction of autophagy resulted in generation of LC3-labeled autophagosomes in the cells. And the amount and distribution of the intracellular autophagosomes could be evaluated by Western blot, and fluorescent microscopy, respectively. However, before these evaluations, 10mM NH $_4$ Cl was added to the cells' culture medium to stop the natural degradation of the autophagosomes inside the cells.

2.6. Evaluation of the Amount of Autophagosomes in LO2 Cells

The amount of autophagosomes in the LO2 cells stably expressing LC3 was evaluated by Western blot. Briefly, cells were lysed and samples were normalized for protein concentration and separated by SDS-PAGE. The transferred PVDF membranes were probed with the primary antibodies (anti-LC3 and anti- β -actin) and then incubated with the secondary antibodies (anti-rabbit IgG). Immunoblots were evaluated using the Odyssey imaging system.

2.7. Examination of the Distribution of Autophagosomes in LO2 Cells

The LO2 cells stably expressing LC3 were examined under a live cell imaging system (Axio Vert.A1, Zeiss, Jena, Germany) equipped a cooled CCD camera (Orca-R², Hamamatsu), definite focus and automated excitation and emission filter wheels controlled by a X-cite SERIES 120Q (LUMEN DYNAMICS) operated by Axio Vision software. Fluorescence was excited through an excitation filter

for FITC (BP 475/40) to visualize the LC3-labeled autophagosomes distributed inside the LO2 cells.

3. RESULTS

3.1. Stable Protein Expression of LC3 in Monoclonal LO2 Cells

Figure 1E and 1F respectively show the immunoblot image and quantitative results of LC3-I/II protein expression in four different monoclones (numbered 3, 4, 5, 7) of LO2 cells transfected with GFP-tagged LC3, and one with pcDNA3 as control. For quantification of the protein expression, the immunoblot data of each monoclones were normalized to that of the house-keeping β -actin. And results from three independent experiments ($n=3$) were presented as mean \pm SD. The results demonstrate that the selected monoclonal cells all stably expressed LC3, as compared to the control. Since cells in No.3 monoclonal expressed the highest level of LC3 than those in the other monoclonal (No.4/5/7), cells from this monoclonal were used for further experiments.

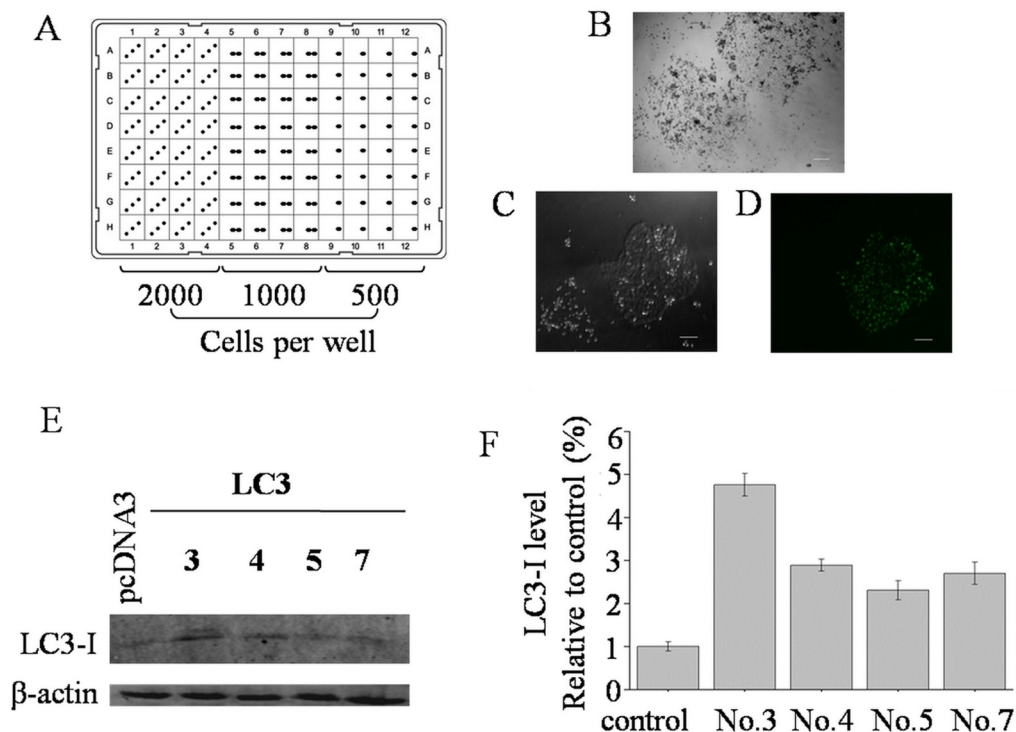


Figure 1: Establishment of LO2 cells with stable expression of GFP-tagged LC3. (A) Cells were seeded in 96-well plates at 2000, 1000, 500 cells per well, respectively, with each cell density in every 4 columns of wells in each plate. (B) Cells formed two or more colonies in the well during the process of G418 selection were discarded. Scale bar equals 50 μ m. (C and D) Cells formed only one clone and stably expressed fluorescent labeled LC3 were selected for further experiment. Scale bar equals 50 μ m. (E) Cells from four monoclonal (Numbered as 3, 4, 5, 7) selections with GFP-LC3 transfection, and transfected with the vehicle of pcDNA3 as control were lysated, and the content of LC3-I was analyzed by Western blot. (F) Quantification of the immunoblots as in (E) for LC3-II in LO2 cells. Values represent the relative levels (Mean \pm SD) of protein expression normalized to β -actin from three independent experiments.

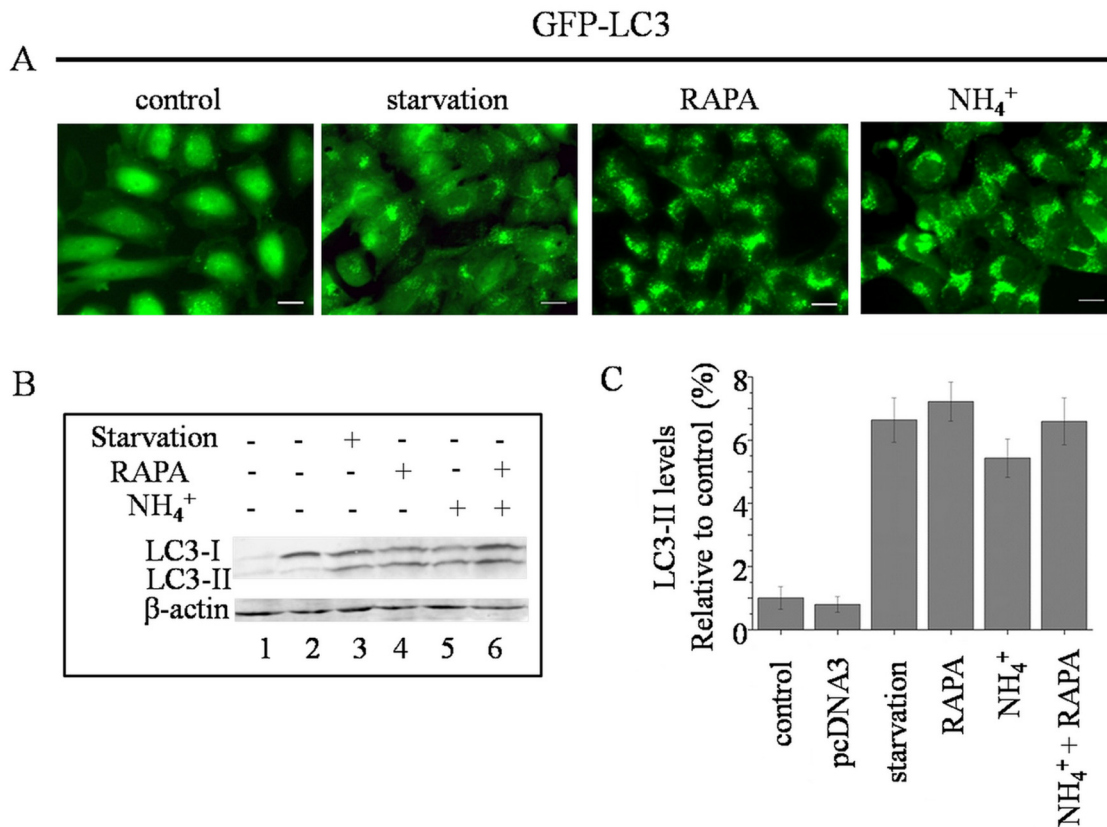


Figure 2: Induction of autophagy in LO2 cells with stable expression of GFP-tagged LC3. **(A)** LO2 cells stably expressing GFP-LC3 were incubated in complete medium (control), amino acid-free medium for (starvation), complete medium with 10 μ M rapamycin (RAPA), or complete medium with 10mM NH₄Cl (NH₄⁺), respectively, for 4h. Scale bar equals 20 μ m. **(B)** Immunoblots of LC3-I/II in LO2 cells with stable transfection of pcDNA3 vehicle, cultured in regular DMEM culture medium (lane1), LO2 cells with stable transfection of GFP-LC3 and cultured in regular DMEM culture medium (lane 2), or DMEM without amino acids and serum (lane 3), DMEM containing 10 μ M rapamycin (lane 4), DMEM containing 10mM NH₄Cl (lane 5), DMEM containing 10 μ M rapamycin+10mM NH₄Cl (lane 6), respectively. **(C)** Quantification of the immunoblots as in **(B)** for LC3-II expression in LO2 cells. Values represent the relative levels (Mean \pm SD) of protein expression normalized to β -actin from three independent experiments.

3.2. Autophagy was Induced in LO2 Cells Stably Expressing GFP-Tagged LC3

As shown in Figure 2, autophagy was induced in LO2 cells stably expressing GFP-LC3, by either serum starvation, or treatment with rapamycin and NH₄Cl for 4h. As compared to the control (left panel in Figure 2A) the number of puncta of GFP-tagged LC3 increased in all cases of treatment including serum starved cells (second panel from the left in Figure 2A), rapamycin treatment (second panel from the right in Figure 2A), NH₄Cl treatment (right panel in Figure 2A). However, the increase of GFP-tagged LC3 puncta was most rapid in cells treated with rapamycin. On the other hand, the increase of GFP-tagged LC3 puncta was due to accumulation rather than generation of GFP-tagged LC3, because NH₄Cl is known to inhibit lysosome-autophagosome fusion and thus reduce autophagosomal degradation, rather than stimulation of new growth of autophagosomes.

Figure 2B shows the immunoblot image of LC3-I/LC3-II expression in LO2 cells either non-transfected and non-treated (control, lane 1), or transfected with pcDNA3 but non-treated (lane 2), transfected with GFP-tagged LC3 and treated with serum starvation (lane 3)/ rapamycin (lane 4, RAPA, 10 μ M)/ NH₄Cl (lane 5, NH₄⁺, 10mM)/ rapamycin plus NH₄Cl (lane 6, RAPA, 10 μ M, NH₄⁺, 10mM), respectively. It appeared that LC3-II was strongly increased as the GFP-LC3 transfected cells were treated with starvation, rapamycin (10 μ M), NH₄Cl (10mM), or rapamycin (10 μ M) plus NH₄Cl (10mM) as compared to the cells non-transfected or transfected with pcDNA3 vehicle (lane 3-6 versus lane 1-2 in Figure 2B). Figure 2C further confirmed quantitatively that LC3-II increased markedly in cells treated with starvation/rapamycin (10mM)/ NH₄Cl (10mM)/ rapamycin (10mM) plus NH₄Cl (10mM) as compared with control/ pcDNA3.

3.3. The Stiffness of the Prepared PDMS Substrate

We prepared PDMS gels of different stiffness by varying the concentration of PDMS crosslinking agent in PDMS polymer suspension. In particular PDMS gels were prepared at three different concentrations of PDMS crosslinking agent in PDMS polymer solution, *i.e.* at 0.2:10, 0.3:10, and 1:10 (w/w), respectively. As shown in Figure 3A, the Young's modulus, or stiffness of the PDMS gel substrate was derived from the force-distance curve measured by atomic force microscopy (AFM). The zero on the x-axis indicated the contact point of the AFM tip on the substrate. When the tip indented into the substrates at a rate of $2.5 \mu\text{m s}^{-1}$, the force exerted on the tip increased exponentially. Thus the Young's modulus was calculated according to Hertz model as described in the Methods. It appeared that the PDMS substrate prepared with PDMS crosslinking agent concentration at 2% (0.2:10 w/w), 3% (0.3:10 w/w), 10% (1:10 w/w) resulted in stiffness of $11 \pm 1.3 \text{ kPa}$, $124 \pm 25 \text{ kPa}$ and $1220 \pm 51 \text{ kPa}$, respectively.

3.4. Substrate Stiffness Influenced the Morphology of LO2 Cells

Figure 3B shows that the LO2 cells grown on substrates with different stiffness were in distinct morphology. The LO2 cells stably transfected with GFP-tagged LC3 were cultured on PDMS substrate of stiffness at 11, 124, and 1220 kPa, as well as plastic

dish, respectively, for 48h. Using phase-contrast microscopy, it could be observed that the cells grown on the stiff PDMS substrate (1220 kPa, lower left panel in Figure 3B) were almost indistinguishable in terms of morphology from those grown on the plastic surface of Petri dish (plastic, lower right panel in Figure 3B). However, the cells grown on increasingly softer PDMS substrate (124 to 11 kPa, upper right panel to upper left panel in Figure 3B) were increasingly less spread and rounded or irregularly shaped.

3.5. Substrate Stiffness had no Effect on the Cell's Synthesis of Autophagosomes

Figure 4 displays the effect of substrate stiffness on the intracellular level of autophagosomes in LO2 cells. The intracellular level of autophagosomes was determined by the endogenous protein level of LC3-II in the cells. LO2 cells stably expressing LC3 were seeded on PDMS substrate with stiffness of 11, 124, 1220 kPa, and plastic substrate of Petri dish, respectively, and cultured for up to 48h in the absence or presence of NH_4Cl ($10 \mu\text{M}$). Subsequently, the cells were lysed and the total intracellular protein levels of LC3 (both LC3-I and LC3-II bands) were measured by Western blot. Panel A and B presented the data for LO2 cells grown on different substrates for 24 and 48h, respectively, with both the immunoblot images of

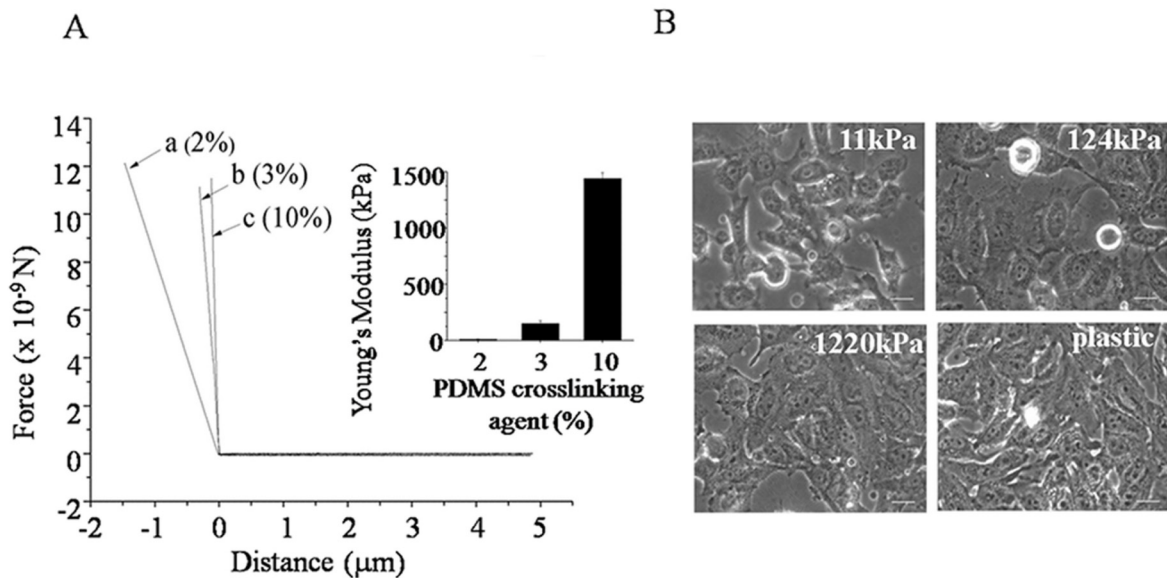


Figure 3: PDMS substrate stiffness and its effect of morphology of LO2 cells. (A) Typical force versus distance curves measured by AFM with approach of a sharp cantilever tip on the PDMS substrate with curing agent/PDMS polymer ratio in weight percentage of 2% (a), 3% (b), 10% (c), respectively. The inset shows the Young's modulus of the PDMS substrate obtained from the AFM indentation experiments. (B) Light microscopy images of LO2 cells with stable expression of GFP-LC3 and grown on PDMS substrate with stiffness of 11, 124, 1220 kPa, respectively, and on plastic surface of Petri dish (plastic). Scale bar equals $20 \mu\text{m}$.

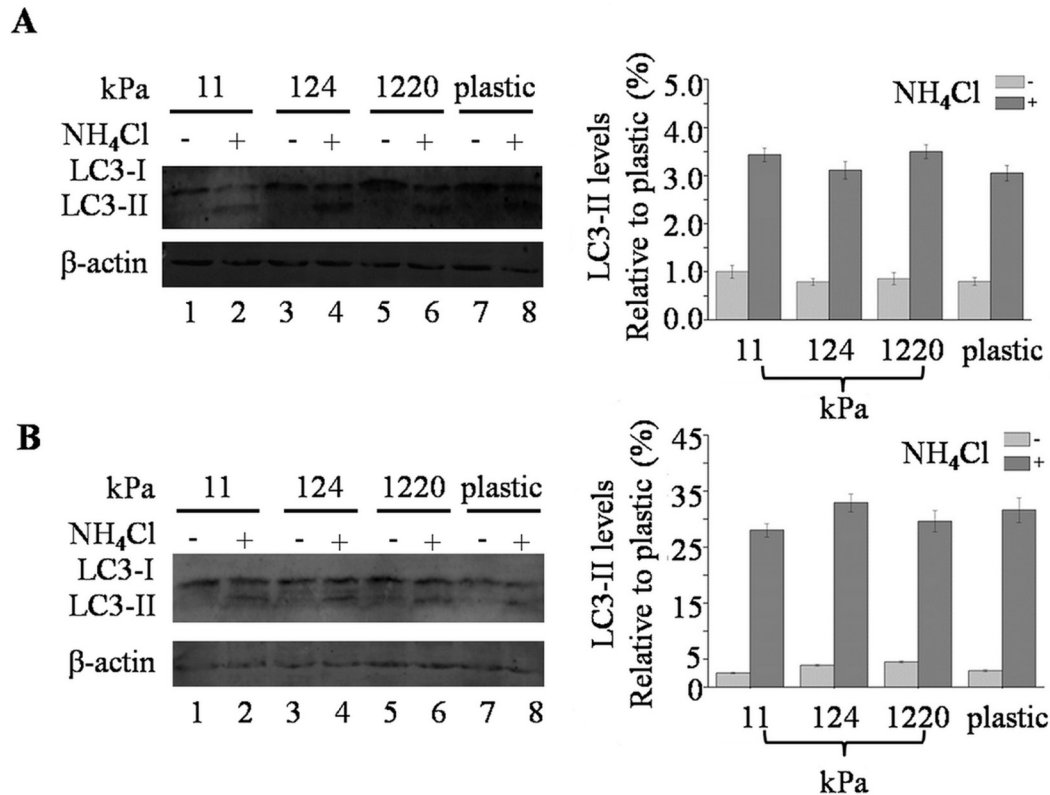


Figure 4: Effect of substrate stiffness on the expression level of LC3 in LO2 cells. **(A)** Immunoblots (left) and quantification (right) of LC3-I/II in LO2 cells with stable transfection of GFP-tagged LC3 and grown on PDMS substrate with stiffness of 11, 124, 1220kPa, plastic surface of Petri dish (plastic), respectively, in the absence or presence of lysosomal inhibitor NH₄Cl for 24h. **(B)** Immunoblots (left) and quantification (right) of LC3-I/II in LO2 cells with stable transfection of GFP-tagged LC3 and grown on PDMS substrate with stiffness of 11, 124, 1220kPa, plastic surface of Petri dish (plastic), respectively, in the absence or presence of lysosomal inhibitor NH₄Cl for 48h. Values represent the relative levels (Mean±SD) of protein expression of LC3-II in LO2 cells normalized to β-actin from three independent experiments.

endogenous LC3 (on the left hand side) and the corresponding quantification of LC3-II protein expression (on the right hand side). It can be seen that regardless of the presence of NH₄Cl, the intracellular protein level of LC3, particularly the LC3-II appeared to be independent on the substrate stiffness, indicating that the substrate stiffness had no effect on the synthesis of autophagosomes in the LO2 cells.

3.6. Substrate Stiffness Altered the Distribution of Autophagosomes in LO2 Cells

Figure 5 shows the distribution of autophagosomes in the LO2 cells stably expressing LC3 when cultured on substrates with different stiffness in the absence or presence of NH₄Cl (10mM). The intracellular autophagosomes were visualized by the GFP-tagged LC3 associated with the autophagosomes under fluorescence microscope. When the cells were cultured for 24h on the substrate with stiffness of 11kPa, 124kPa, 1220kPa, and plastic surface of Petri dish, respectively (panel A from the left to right hand image),

the GFP-tagged LC3 appeared as a diffusive cytoplasmic pool with only a few small punctate autophagosomes emerged on the edge of the cell. This indicates that the substrate stiffness seemed unable to influence the distribution of autophagosomes inside the LO2 cells when cultured on the substrate for less than 24h.

However, as shown in the panel C, when the cells were cultured on the substrates for 48h, a large number of punctate autophagosomes localized around the peripheral of nucleus of the cells in all cases. More interestingly, the intracellular autophagosomes were increasingly less diffusive and more clustered into spheres around the nucleus as the substrate became increasingly softer (panel C from the right to left hand image). And at 48h the cells grown on stiff PDMS substrate (1220kPa) and plastic surface of Petri dish (plastic) still exhibited dispersed autophagosomes throughout the cytoplasm. When cultured in the presence of NH₄Cl, the substrate stiffness dependent phenomenon of accumulation and spherical clustering

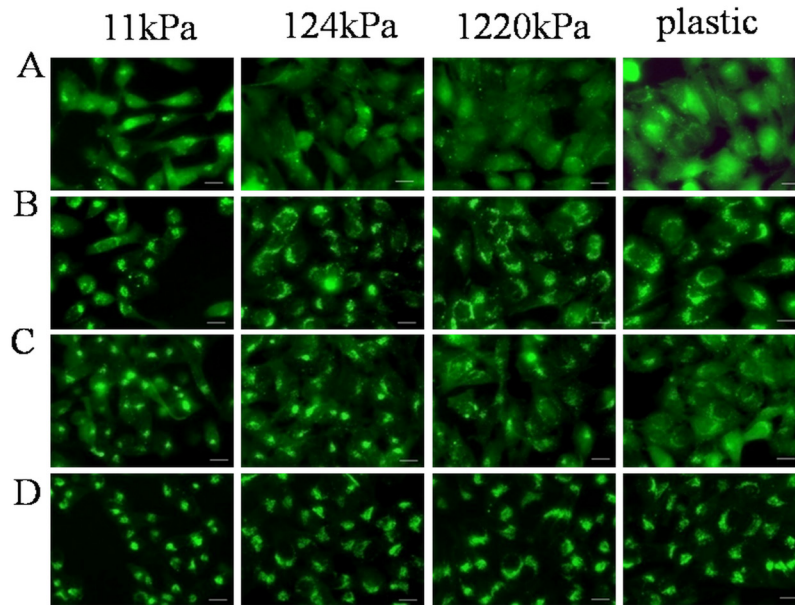


Figure 5: Effect of substrate stiffness on the distribution of autophagosomes in LO2 cells with stable transfection of GFP-tagged LC3. (A, C) From left to right, fluorescent microscopy images of autophagosomes labeled by GFP-LC3 in LO2 cells grown on PDMS substrate with stiffness of 11, 124, 1220kPa, plastic surface of Petri dish (plastic) for 24h (A) or 48h (C). Scale bar equals 20 μ m. (B, D) Same as (A) and (C) except that the cells were cultured in the presence of 10mM NH₄Cl. Scale bar equals 20 μ m.

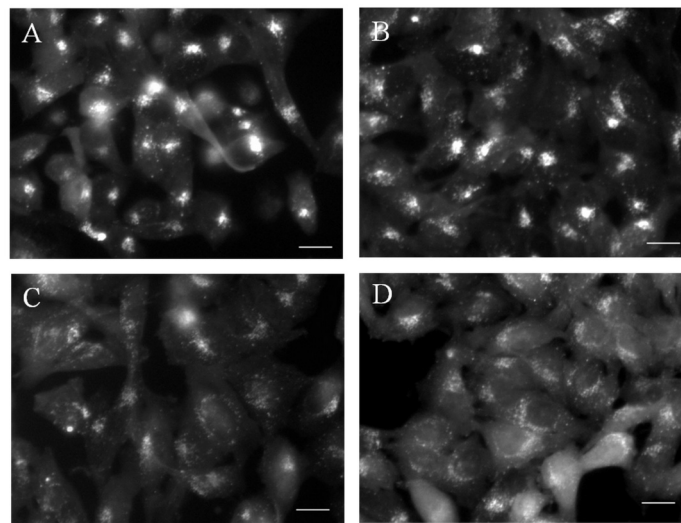


Figure 6: Zoom-in images of GFP-LC3 labeled autophagosomes in LO2 cells. LO2 cells cultured for 48h on PDMS substrate with stiffness of 11kPa (A), 124 kPa (B), 1220kPa(C), and plastic surface of Petri dish (D).

of autophagosomes seemed to be enhanced at both 24 and 48h (panel B and D). Figure 6 displays zoom-in images to show more details of the increasing spherical clustering of autophagosomes inside the LO2 cells as the substrate became increasingly softer (D to A corresponding to the substrate stiffness from plastic to 1220kPa, 124kPa, and 11kPa, respectively). This observed phenomenon was further quantified by counting the number of cells either with or without autophagosomes accumulated around the nuclei (perinuclear accumulation). The results indicate that

the difference in the number of cells with perinuclear autophagosomes accumulation increased from 17 ± 3 to 117 ± 15 (>6 fold) when the stiffness changed from 1220 to 11kPa ($p < 0.05$) (Figure 7).

4. DISCUSSION

In this study, we used a classical method to measure autophagic flux by monitoring the turnover of LC3 inside the LO2 cells. It is well-known that the amount of LC3-II usually correlates well with the number of autophagosomes, or more precisely in

theory, the amount of autophagic membrane labeled with LC3-II [25]. Although there are many autophagy proteins known to participate in the process of autophagy, only a few of them would turn up in autolysosomes, among which LC3 would not only appear throughout the process of autophagy, but also could appear in autolysosomes, thus LC3 could act as a specific marker of autophagy [25, 26]. However, LC3 itself could be a protein prone to aggregation, mainly due to over expression by transient transfection. Therefore, it is highly recommended to use cells stably expressing transfected GFP-LC3 because such cells do not possess aggregated LC3 [27].

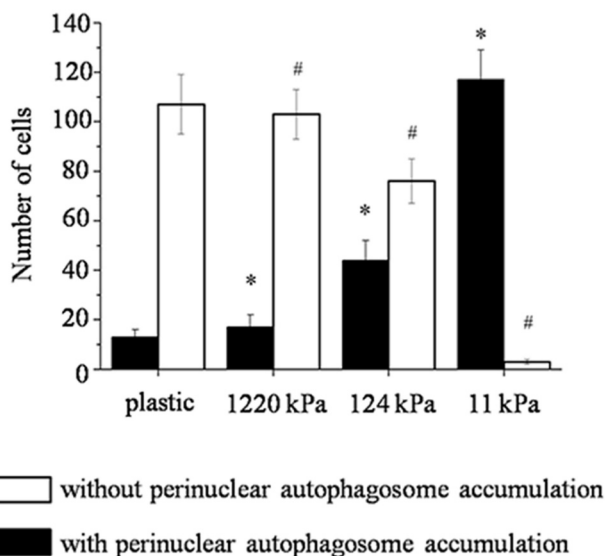


Figure 7: Summary of perinuclear autophagosome accumulation in LO2 cells. In each experiment, at least 120 LO2 cells stably expressing GFP-LC3 grown on PDMS substrate with stiffness of 11, 124, 1220kPa, plastic surface of Petri dish (plastic) were analyzed. Data are shown as mean \pm SD of triplicate experiments (*, $p < 0.05$ vs. plastic with perinuclear autophagosome accumulation; #, $p < 0.05$ vs. plastic without perinuclear autophagosome accumulation, $n = 3$).

There are two conventional methods for establishing cells stably expressing GFP-tagged LC3. One is to plate cells in 24-well cell culture plate after transfection of GFP-tagged LC3 for 48h, and then further culture the cells in the medium containing G418. Depending on the cell type and concentration of G418 in the medium, the transfected cells in culture would form a large positive clone after 9 or more days. At that point, a cloning cylinder is placed to encircle the cells and afterwards harvest the cells by trypsinization or EDTA inside the cylinder. Subsequently the harvested cells were plated into 96-well cell culture plates to expand the cultivation. The other follows the same first

few steps as described above, but differs in the way to select a positive clone. It selects the positive clone under a microscope in a super-clean bench, and scrapes off the negative clones at high magnification. Then the positive clone is digested and expanded in culture.

However, the above two methods have some common problems. For instance, both are very tedious to operate, easy to cause contamination, as well as difficult to ensure the monoclonal state of the selected cells. The method we used, as described in Methods, was simple, and high throughput, which enabled selection of multiple wells of positive cells with ensured monoclonal state at one time.

Rapamycin is known to induce autophagy by inhibiting mTOR, a protein kinase that regulates cell growth and protein synthesis, and the formation of autophagosomes [28, 29]. The dynamic processes of autophagosome synthesis, delivery of autophagic substrates to the lysosome, and degradation of autophagic substrates inside the lysosome are often termed "autophagic flux" [30]. Since the number of autophagosome is not only dependent on the production of autophagosomes but also the degradation of them. Therefore, to accurately study the "autophagic flux" requires exclusion of the confounding factor of autophagosome degradation. For this purpose, NH_4Cl that is a known inhibitor of lysosomal proteolysis was added to the culture medium in which the cells were grown. As shown in Figure 4, the time-dependent accumulation of LC3-II in LO2 cells was markedly greater when the cells were exposed to NH_4Cl as compared to those not exposed to it, indicating effective inhibition of the degradation of autophagosomes in the cells.

In this study, we used PDMS gel as substrate to culture LO2 cells so that the stiffness of the substrate could be easily varied in order to examine the effects of substrate stiffness on autophagy in LO2 cells. PDMS is a biocompatible material that has been widely used in studies of cellular behaviors, in particular the interaction behavior between cells and the substrate, largely due to its availability and convenience for manipulation of its mechanical properties [31, 32]. Using PDMS as cell culture substrate, it has been extensively demonstrated that the stiffness of substrate regulates a broad range of cell functions including growth, motility, and viability. However, it has not been studied whether the substrate stiffness would have any

effect on the cell's autophagy, which may be important in understanding tumor formation that is associated with both tissue stiffening and autophagy.

Our data show that the intracellular level of LC3-II in LO2 cells was not affected by the substrate stiffness whether cultured for 24 or 48h, with or without NH₄Cl treatment (Figure 4). This strongly suggest that the substrate stiffness does not influence the synthesis or the degradation of the endogenous autophagosomes, thus ECM stiffness may not well be a determinant of the autophagic level in the cell. However, the structure and distribution of intracellular autophagosomes were strongly dependent on the substrate stiffness. On stiff substrate the autophagosomes were scattered throughout the cytoplasm, without particular structural characteristics. In contrast, on the soft substrate the autophagosomes quickly translocated towards the nucleus and accumulated into spherical bodies around the nucleus. The underlying mechanisms of the effect of substrate stiffness on the distribution of autophagosomes inside the cell remain to be elucidated. Nevertheless, we may speculate that this phenomenon is probably, at least in a large part, due to substrate stiffness induced modification of structural organization of the cytoskeleton, especially the microtubule filament network. In our observation the clustered spherical bodies of LC3 mostly locate in the region around the microtubule-organizing center (MTOC).

It is known that microtubule network provides an important function as transport tracks along which intracellular organelles such as autophagosomes move and transport cargos from one place to another inside the cell. This network system, however, is not static, instead is highly dynamic. Throughout the life cycle of the cell the cytoskeleton system undergoes constant rearrangement. The microtubule filaments in the living cell are of no exception, constantly change their length and orientation as they shift between the slow growth phase to rapid shrinkage phase at the plus ends, depending on the rate of polymerization of pure tubulin [33]. The conversion from growing to shrinking is called catastrophe, whereas the reverse is called rescue. And the balance between catastrophe and rescue constitutes the dynamic instability of the microtubule structure in the living cell [34, 35]. Furthermore, this highly instable intracellular microtubule structure is known to be influenced by both the physical and chemical cues from the ECM [36-38]. For example, increase of substrate stiffness is known to elevate the intracellular tension. As predictable by the well-known

tensegrity model of cell mechanics, the microtubules in the cells of great tension must be also stiffer and more stable, just like the cables of a tensed tent. And it is reasonable to assume that the organelles such as autophagosomes would move faster and more easily along stiff and stable microtubule filaments as compared to moving along floppy and unstable ones. In such perspective, it is not surprising to see uniformly dispersed autophagosomes in cells grown on stiff substrate, but localized and clustered autophagosomes in cells grown on soft substrate.

5. CONCLUSION

The primary finding of this study is that under the condition of *in vitro* culture the substrate stiffness had no effect on the intracellular synthesis of autophagosomes, but did influence the intracellular distribution of the autophagosomes in LO2 cells that stably expressed GFP-tagged LC3. On stiff substrate, the autophagosomes tended to disperse throughout the cytoplasm of the cells. In contrast, on soft substrate the autophagosomes tended to aggregate or cluster into spherical bodies around the nucleus. This finding serves as a proof of concept that the pathological stiffening of liver tissue occurring during progression of liver fibrosis and cirrhosis might not simply cause abnormal autophagy by influencing the synthesis of intracellular autophagosomes, but instead cause abnormal function of autophagy by modifying the distribution of intracellular autophagosomes. What is important to be studied in future is the motion dynamics of autophagosomes in relation to microtubule structural remodeling and the exact functional role of autophagosomes distribution in regulation of autophagy during health and disease process.

ACKNOWLEDGEMENT

This research is partially supported by grants from National Natural Science Foundation of China (Grant No. 11172340); Office for Talent Recruitment of Jiangsu Province, China (Double Talent Plan Grant No. SRCB-2012-39); Bureau of Science and Technology of Changzhou Municipality, Jiangsu Province, China (Key Laboratory Grant No. CM20133005); Graduate Student Research and Innovation Program for General Universities of Jiangsu Province (CXZZ13_07)

REFERENCES

- [1] Forner A, Llovet JM, Bruix J. Hepatocellular carcinoma. *Lancet* 2012; 379(9822): 1245-55. [http://dx.doi.org/10.1016/S0140-6736\(11\)61347-0](http://dx.doi.org/10.1016/S0140-6736(11)61347-0)

- [2] Bruix J, Sherman M. Management of hepatocellular carcinoma: an update. *Hepatology* 2011; 53(3): 1020-2. <http://dx.doi.org/10.1002/hep.24199>
- [3] EASL-EORTC clinical practice guidelines: management of hepatocellular carcinoma. *J Hepatol* 2012; 56(4): 908-43. <http://dx.doi.org/10.1016/j.jhep.2011.12.001>
- [4] Georges PC, Hui JJ, Gombos Z, McCormick ME, Wang AY, Uemura M, *et al.* Increased stiffness of the rat liver precedes matrix deposition: implications for fibrosis. *Am J Physiol-Gastr L* 2007; 293(6): G1147-54. <http://dx.doi.org/10.1152/ajpgi.00032.2007>
- [5] Yin M, Talwalkar JA, Glaser KJ, Manduca A, Grimm RC, Rossman PJ, *et al.* Assessment of hepatic fibrosis with magnetic resonance elastography. *Clin Gastroenterol H* 2007; 5(10): 1207-13 e2.
- [6] Beningo KA, Wang Y-L. Flexible substrata for the detection of cellular traction forces. *Trends Cell Biol* 2002; 12(2): 79-84. <http://dx.doi.org/10.1152/ajpgi.00032.2007>
- [7] Pelham RJ, Jr., Wang Y. Cell locomotion and focal adhesions are regulated by substrate flexibility. *P Natl Acad Sci USA* 1997; 94(25): 13661-5. <http://dx.doi.org/10.1073/pnas.94.25.13661>
- [8] Yeung T, Georges PC, Flanagan LA, Marg B, Ortiz M, Funaki M, *et al.* Effects of substrate stiffness on cell morphology, cytoskeletal structure, and adhesion. *Cell Motil Cytoskel* 2005; 60(1): 24-34. <http://dx.doi.org/10.1002/cm.20041>
- [9] Roos E. Cellular adhesion, invasion and metastasis. *Bba-Rev Cancer* 1984; 738(4): 263-84. [http://dx.doi.org/10.1016/0304-419X\(83\)90008-2](http://dx.doi.org/10.1016/0304-419X(83)90008-2)
- [10] Huang S, Ingber DE. Cell tension, matrix mechanics, and cancer development. *Cancer Cell* 2005; 8(3): 175-6. <http://dx.doi.org/10.1016/j.ccr.2005.08.009>
- [11] Rautou P-E, Mansouri A, Lebrec D, Durand F, Valla D, Moreau R. Autophagy in liver diseases. *Hepatology* 2010; 53: 1123-34. <http://dx.doi.org/10.1016/j.jhep.2010.07.006>
- [12] Adhami F, Liao G, Morozov YM, Schloemer A, Schmithorst VJ, Lorenz JN, *et al.* Cerebral ischemia-hypoxia induces intravascular coagulation and autophagy. *Am J Pathol* 2006; 169(2): 566-83. <http://dx.doi.org/10.2353/ajpath.2006.051066>
- [13] Axe EL, Walker SA, Manifava M, Chandra P, Roderick HL, Habermann A, *et al.* Autophagosome formation from membrane compartments enriched in phosphatidylinositol 3-phosphate and dynamically connected to the endoplasmic reticulum. *J Cell Biol* 2008; 182(4): 685-701. <http://dx.doi.org/10.1083/jcb.200803137>
- [14] Dunn W. Studies on the mechanisms of autophagy: maturation of the autophagic vacuole. *J. Cell Biol* 1990; 110(6): 1935-45. <http://dx.doi.org/10.1083/jcb.110.6.1935>
- [15] Singh R, Kaushik S, Wang Y, Xiang Y, Novak I, Komatsu M, *et al.* Autophagy regulates lipid metabolism. *Nature* 2009; 458(7242): 1131-5. <http://dx.doi.org/10.1038/nature07976>
- [16] Deretic V, Levine B. Autophagy, Immunity, and Microbial Adaptations. *Cell Host Microbe* 2009; 5(6): 527-49. <http://dx.doi.org/10.1016/j.chom.2009.05.016>
- [17] Ding ZB, Shi YH, Zhou J, Qiu SJ, Xu Y, Dai Z, *et al.* Association of autophagy defect with a malignant phenotype and poor prognosis of hepatocellular carcinoma. *Cancer Res* 2008; 68(22): 9167-75. <http://dx.doi.org/10.1158/0008-5472.CAN-08-1573>
- [18] Yin X-M, Ding W-X, Gao W. Autophagy in the liver. *Hepatology* 2008; 47(5): 1773-85. <http://dx.doi.org/10.1002/hep.22146>
- [19] Cardinal J, Pan P, Dhupar R, Ross M, Nakao A, Lotze M, *et al.* Cisplatin prevents high mobility group box 1 release and is protective in a murine model of hepatic ischemia/reperfusion injury. *Hepatology* 2009; 50(2): 565-74. <http://dx.doi.org/10.1002/hep.23021>
- [20] Rubinsztein DC, Gestwicki JE, Murphy LO, Klionsky DJ. Potential therapeutic applications of autophagy. *Nat Rev Drug Discov* 2007; 6(4): 304-12. <http://dx.doi.org/10.1038/nrd2272>
- [21] Schrader J, Gordon-Walker TT, Aucott RL, van Deemter M, Quaas A, Walsh S, *et al.* Matrix stiffness modulates proliferation, chemotherapeutic response, and dormancy in hepatocellular carcinoma cells. *Hepatology* 2011; 53(4): 1192-205. <http://dx.doi.org/10.1002/hep.24108>
- [22] Rautou P-E, Mansouri A, Lebrec D, Durand F, Valla D, Moreau R. Autophagy in liver diseases. *J Hepatol* 2010; 53(6): 1123-34. <http://dx.doi.org/10.1016/j.jhep.2010.07.006>
- [23] Hutter JL, Bechhoefer J. Calibration of atomic - force microscope tips. *Rev Sci Instrum* 1993; 64(7): 1868-73. <http://dx.doi.org/10.1063/1.1143970>
- [24] Lin L-Y, Kim D-E. Measurement of the elastic modulus of polymeric films using an AFM with a steel micro-spherical probe tip. *Polym Test* 2012; 31(7): 926-30. <http://dx.doi.org/10.1016/j.polymertesting.2012.06.012>
- [25] Kabeya Y, Mizushima N, Ueno T, Yamamoto A, Kirisako T, Noda T, *et al.* LC3, a mammalian homologue of yeast Apg8p, is localized in autophagosomal membranes after processing. *EMBO J* 2000; 19(21): 5720-8. <http://dx.doi.org/10.1093/emboj/19.21.5720>
- [26] Mizushima N, Levine B, Cuervo AM, Klionsky DJ. Autophagy fights disease through cellular self-digestion. *Nature* 2008; 451(7182): 1069-75. <http://dx.doi.org/10.1038/nature06639>
- [27] Kuma A, Matsui M, Mizushima N. LC3, an autophagosome marker, can be incorporated into protein aggregates independent of autophagy: caution in the interpretation of LC3 localization. *Autophagy* 2007; 3(4): 323-8. <http://dx.doi.org/10.4161/auto.4012>
- [28] Schmelzle T, Hall MN. TOR, a central controller of cell growth. *Cell* 2000; 103(2): 253-62. [http://dx.doi.org/10.1016/S0092-8674\(00\)00117-3](http://dx.doi.org/10.1016/S0092-8674(00)00117-3)
- [29] Ravikumar B, Vacher C, Berger Z, Davies JE, Luo S, Oroz LG, *et al.* Inhibition of mTOR induces autophagy and reduces toxicity of polyglutamine expansions in fly and mouse models of Huntington disease. *Nat Genet* 2004; 36(6): 585-95. <http://dx.doi.org/10.1038/ng1362>
- [30] Mizushima N, Yoshimori T, Levine B. Methods in Mammalian Autophagy Research. *Cell* 2010; 140(3): 313-26. <http://dx.doi.org/10.1016/j.cell.2010.01.028>
- [31] Yim EK, Reano RM, Pang SW, Yee AF, Chen CS, Leong KW. Nanopattern-induced changes in morphology and motility of smooth muscle cells. *Biomaterials* 2005; 26(26): 5405-13. <http://dx.doi.org/10.1016/j.biomaterials.2005.01.058>
- [32] Toworfe GK, Composto RJ, Adams CS, Shapiro IM, Ducheyne P. Fibronectin adsorption on surface-activated poly(dimethylsiloxane) and its effect on cellular function. *J Biomed Mater Res A* 2004; 71(3): 449-61. <http://dx.doi.org/10.1002/jbm.a.30164>
- [33] Mitchison T, Kirschner M. Dynamic instability of microtubule growth. *Nature* 1984; 312(5991): 237-42. <http://dx.doi.org/10.1038/312237a0>
- [34] Cassimeris L, Pryer NK, Salmon ED. Real-time observations of microtubule dynamic instability in living cells. *J. Cell Biol.* 1988; 107(6 Pt 1): 2223-31. <http://dx.doi.org/10.1083/jcb.107.6.2223>

-
- [35] Sammak PJ, Borisy GG. Direct observation of microtubule dynamics in living cells. *Nature* 1988; 332(6166): 724-6.
<http://dx.doi.org/10.1038/332724a0>
- [36] Kirschner M, Mitchison T. Beyond self-assembly: from microtubules to morphogenesis. *Cell* 1986; 45(3): 329-42.
[http://dx.doi.org/10.1016/0092-8674\(86\)90318-1](http://dx.doi.org/10.1016/0092-8674(86)90318-1)
- [37] Karsenti E. Mitotic spindle morphogenesis in animal cells. *Semin. Cell. Biol.* 1991; 2(4): 251-60.
- [38] Hyman AA, Karsenti E. Morphogenetic properties of microtubules and mitotic spindle assembly. *Cell* 1996; 84(3): 401-10.
[http://dx.doi.org/10.1016/S0092-8674\(00\)81285-4](http://dx.doi.org/10.1016/S0092-8674(00)81285-4)

Received on 28-03-2015

Accepted on 14-04-2015

Published on 29-04-2015

<http://dx.doi.org/10.15379/2409-3394.2015.02.01.1>© 2015 Xu *et al.*; Licensee Cosmos Scholars Publishing House.

This is an open access article licensed under the terms of the Creative Commons Attribution Non-Commercial License

(http://creativecommons.org/licenses/by-nc/3.0/), which permits unrestricted, non-commercial use, distribution and reproduction in any medium, provided the work is properly cited.